NanoSIMS imaging: an approach for visualizing and quantifying lipids in cells and tissues

Cuiwen He,[1] Loren G Fong,[1] Stephen G Young,[1,2] Haibo Jiang[3]

[1]Departments of Medicine, David Geffen School of Medicine, University of California, Los Angeles, California, USA
[2]Departments of Human Genetics, David Geffen School of Medicine, University of California, Los Angeles, California, USA
[3]Centre for Microscopy, Characterisation, and Analysis, The University of Western Australia, Perth, Western Australia, Australia

Correspondence to
Dr Haibo Jiang, Centre for Microscopy, Characterisation, and Analysis, The University of Western Australia, Perth, WA 6009, Australia; haibo.jiang@uwa.edu.au

Accepted 27 August 2016
Published Online First 28 October 2016

ABSTRACT

Over the past few decades, several approaches have been used to image lipids in cells and tissues, but most have limited spatial resolution and sensitivity. Here, we discuss a relatively new approach, nanoscale secondary ion mass spectrometry imaging, that makes it possible to visualize lipids in cells and tissues in a quantitative fashion and with high spatial resolution and high sensitivity.

INTRODUCTION

High-resolution imaging of lipids in cells and tissues has been challenging.[1] Fluorescently tagged lipids, for example, BODIPY-labeled lipids,[2] have been widely used to image lipids in live cells and have proven to be very useful.[3 4] However, with this approach, there are often concerns about the biochemical properties of the tagged lipids (ie, that the tissue localization and/or metabolism of the tagged lipids differ from unmodified lipids). For this reason, label-free imaging of lipids would be preferable—at least for certain applications. Recent studies have used 2 approaches for imaging label-free lipids: Raman spectroscopy[5 6] and SIMS.[7] Raman spectroscopy detects the vibrational information from the sample, which is specific to the chemical bonds (eg, C=O, C–H, and CH_2) and to the symmetry of molecules. The spontaneous Raman signals are typically very low, but the sensitivity of Raman spectroscopy has improved in recent years, making it possible to obtain high-resolution images of lipid bilayers[8] and to detect certain covalent modifications of lipids.[9] Raman spectroscopy uses these signals, such as the hydrocarbon chain vibration of CH_2 and CH_3 groups and C-C and C-H stretching modes, for detecting different types of lipids, but the ability to identify specific lipid species unambiguously is limited. SIMS, particularly time-of-flight SIMS, generates fragmented secondary ions that can be used to visualize lipids in tissues,[10] but the spatial resolution and sensitivity of this approach is rather limited, such that it cannot be used to image lipids within subcellular structures.

To improve the specificity of Raman spectroscopy for identifying lipids, deuterium-labeled lipids have been used.[11] The C–D bonds have a unique peak (~2100/cm) in the Raman spectrum,[12] but only a single lipid molecule can be visualized. On the other hand, secondary ion mass spectrometry (SIMS) can be used to detect deuterium and other stable isotopes simultaneously, making it possible to visualize and track several lipids—each labeled with a different isotope. The nanoscale SIMS (NanoSIMS, CAMECA, France) instruments have high sensitivity and remarkably good spatial resolution, making it possible to image lipids in different cellular organelles.[13] Here, we review methods for imaging lipids by NanoSIMS and suggest several potential applications.

CORRELATIVE NANOSIMS AND BACKSCATTERED ELECTRON IMAGING

NanoSIMS imaging was initially used mainly for measuring isotopic ratios and trace elements within geochemistry and material science departments, but beginning in 2004, this approach has attracted interest from biologists.[14] For biologists, the NanoSIMS instrument has proven useful for visualizing the fate of stable isotope-labeled molecules in cells and tissues.[15–17] The NanoSIMS instrument bombards a section of cells or tissues with a primary ion beam (O^- or Cs^+), and then collects and identifies secondary ions based on mass-to-charge ratios. NanoSIMS instruments achieve high spatial resolution, high mass resolution, and high sensitivity, making it feasible to visualize stable isotope-labeled lipids at a subcellular resolution. Indeed, Frisz *et al*[18 19] used NanoSIMS to visualize the microdomain distribution of ^{18}O-labeled cholesterol and ^{15}N-labeled sphingolipids on the plasma membrane of NIH 3T3 fibroblasts. A key advantage of NanoSIMS imaging of lipids is that it does not require using lipids that have been modified with bulky fluorescent tags. Stable isotopes have little or no effect on the biological properties of lipids, and a large variety of stable isotope-labeled lipids are available from commercial vendors.

For imaging lipids in cells and tissues, we have adopted a novel approach called *correlative NanoSIMS and backscattered electron imaging* (CNBEI). This approach is superior to NanoSIMS alone. The ion-induced secondary electron signal from the NanoSIMS is able to provide some topographical information regarding the surface of the sample; however, it does not provide high-resolution morphological information resulting from atomic mass contrast in biological samples stained with heavy metals.

To cite: He C, Fong LG, Young SG, *et al*. *J Investig Med* 2017;**65**:669–672.

CNBEI is able to generate, from the very same sections, both high-resolution morphological information (backscattered electron (BSE) imaging) and chemical information (NanoSIMS). CNBEI has proven useful for visualizing stable isotope-labeled lipids in mouse tissues. In a typical experiment, we administer stable isotope-labeled lipids to the mouse and then prepare tissue sections for imaging studies. Initially, we examine tissue sections by BSE imaging with a scanning electron microscopy, which provides high-resolution images of cells (allowing visualization of cellular organelles). Once subcellular morphology has been defined, we image the same tissue section by the NanoSIMS. In this way, we can correlate high-resolution morphological data from BSE images with the chemical information provided by the NanoSIMS. We recently used this correlative imaging approach to document margination of ^{13}C-labeled triglyceride-rich lipoproteins (TRLs) along the luminal surface of capillary endothelial cells (figure 1).[20 21]

In a typical NanoSIMS imaging study, millions of secondary ions are collected and used to construct a high-resolution image. Images can be created solely from the release of single secondary ions from the tissue section (eg, $^{1}H^{-}$, $^{2}H^{-}$, $^{12}C^{-}$, $^{13}C^{-}$) or from the *ratio* of two secondary ions (eg, $^{13}C^{-}$:$^{12}C^{-}$). All of the secondary ions that are used to create images are available for quantitative analyses. In recent studies, we used NanoSIMS imaging data to quantify the impact of GPIHBP1 deficiency on the transport of ^{13}C-labeled lipids from the plasma compartment to surrounding parenchymal cells. GPIHBP1 is an endothelial cell protein that shuttles a triglyceride hydrolase, lipoprotein lipase (LPL), from the interstitial spaces to the capillary lumen. LPL hydrolyzes the triglycerides in TRLs, releasing fatty acids that are taken up and used by surrounding parenchymal cells.[22] In the setting of GPIHBP1 deficiency, LPL never reaches the lumen of capillaries and instead remains mislocalized within the interstitial spaces, interfering with the lipolytic processing of TRLs; consequently, there is an accumulation of unprocessed TRLs in the plasma and reduced delivery of lipid nutrients to parenchymal cells. To quantify the extent of the metabolic defect in GPIHBP1 deficiency, we fed wild-type and GPIHBP1-deficient mice ^{13}C-labeled fatty acids for 4 days and then sacrificed the mice and prepared sections of brown adipose tissue (BAT) and heart for NanoSIMS imaging (figure 2). In the tissue sections from GPIHBP1 knockout mice (*Gpihbp1*$^{-/-}$), large amounts of ^{13}C were present inside capillaries, revealing an accumulation of unprocessed TRLs in the bloodstream. Not surprisingly, the amount of ^{13}C reaching cytosolic lipid droplets was reduced, reflecting diminished delivery of ^{13}C lipids from the bloodstream to the parenchymal cells (figure 2C, F).[20] The ^{13}C/^{12}C ratio in BAT lipid droplets in wild-type mice was 2.2%, 51.7% higher than the ratio in the BAT of *Gpihbp1*$^{-/-}$ mice (1.45%). Similar findings were apparent in the heart. The ^{13}C/^{12}C ratio in cardiomyocyte lipid droplets in wild-type mice was 1.8% versus only 1.46% in cardiomyocyte lipid droplets in *Gpihbp1*$^{-/-}$ mice. In addition, the number of lipid droplets in cardiomyocytes was greater in wild-type mice than in *Gpihbp1*$^{-/-}$ mice.

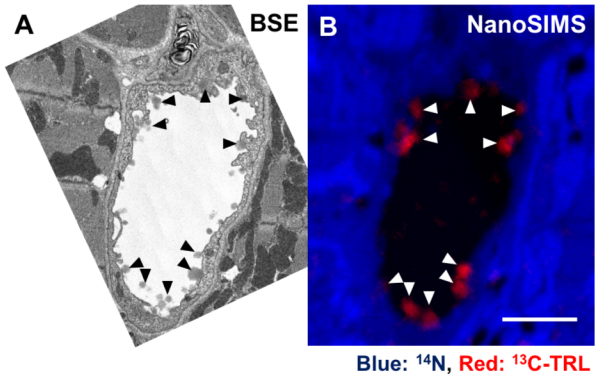

Figure 1 High-resolution images of lipids with CNBEI. A wild-type mouse was injected intravenously with ^{13}C-labeled TRLs and then sacrificed 15 min later. (A) A BSE image of a heart section revealed darkly staining spherical particles (arrowheads) along the luminal surface of a capillary. (B) NanoSIMS image of the ^{13}C/^{12}C ratio (red, ranging from 1.1% to 2.2%) and ^{14}N (blue) —revealing that the spherical particles along the capillary lumen (arrowheads) in the BSE image were enriched in ^{13}C, proving that those particles represented ^{13}C-TRLs that had marginated along the surface of capillary endothelial cells. Scale bar, 2 μm. Reproduced, with permission, from Fong *et al*.[22] BSE, backscattered electron; CNBEI, correlative NanoSIMS and backscattered electron imaging; NanoSIMS, nanoscale secondary ion mass spectrometry; TRL, triglyceride-rich lipoprotein.

POTENTIAL APPLICATIONS OF CNBEI

The CNBEI approach provides many opportunities for better understanding lipid movement in cells and tissues. For example, at the current time, the mechanisms by which the fatty acid products of TRL processing traverse capillaries (in the direction of parenchymal cells) are poorly understood. One possibility is that fatty acids 'diffuse' along endothelial cell membranes and move across endothelial cells in channels.[23] Another possibility is that most of the fatty acids move across endothelial cells in transcytotic vesicles—perhaps attached to CD36 (an integral membrane protein thought to be important for fatty acid transport).[24] Another possibility is that the fatty acids move across the cytoplasm of endothelial cells. During the past year, we have initiated NanoSIMS studies to visualize the movement of lipids across capillary endothelial cells. Using the CNBEI approach, we uncovered occasional examples of TRLs inside capillary endothelial cells and rare examples of intact TRLs that had moved across endothelial cells into the subendothelial space. However, we doubt that the movement of intact TRL *particles* across endothelial cells plays a quantitatively important role in transporting lipids to surrounding parenchymal cells. In our initial studies, we were not successful in imaging the movement of *free fatty acids* across endothelial cells. We suspect that the fixation methods that we employed were suboptimal for fixing free fatty acids and that we may have examined tissues at time points when most of the fatty acids had already traversed endothelial cells. In future studies, by optimizing methods for tissue fixation, we anticipate being able to visualize the movement of fatty acids across endothelial cells, thereby gaining clues regarding the cellular mechanisms for lipid transport across endothelial cells. An early goal will be to investigate the role of CD36 in lipid transport across endothelial cells. A role for CD36 in the uptake of lipids by cardiomyocytes and adipocytes is well documented,[24] but the

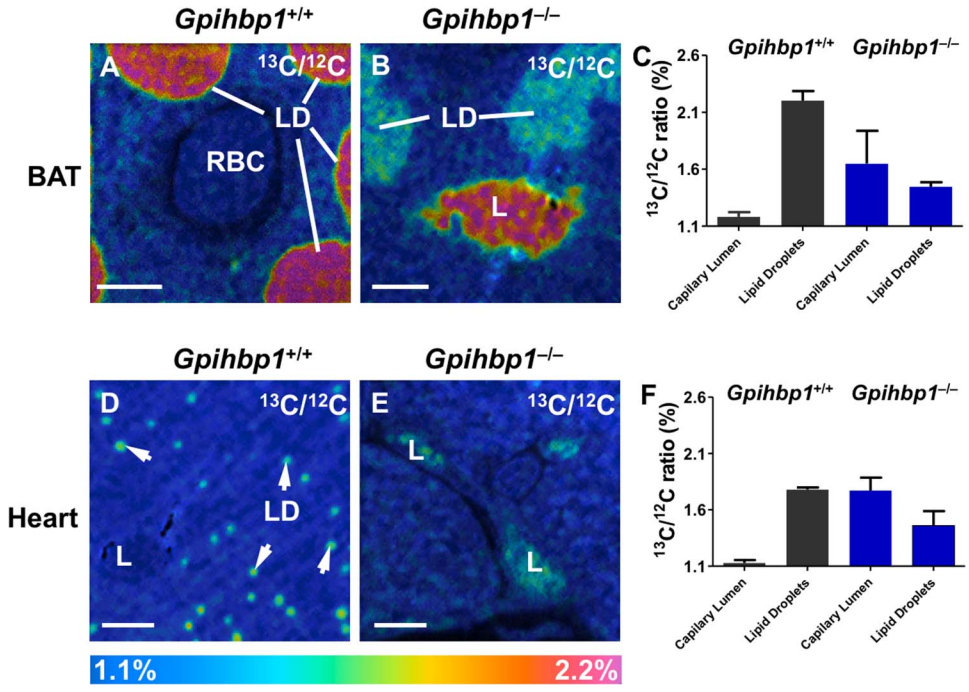

Figure 2 Using NanoSIMS imaging to quantify the reduced delivery of lipids from the plasma compartment to parenchymal cells in the setting of GPIHBP1 deficiency. Wild-type mice and GPIHBP1-deficient mice (Gpihbp1−/−) were fed ^{13}C-fatty acids for 4 days and then sacrificed. (A, B, D and E): ^{13}C/^{12}C NanoSIMS images of sections of BAT (A and B) and heart (D and E) from Gpihbp1+/+ and Gpihbp1 −/−mice. (C and F) Quantification of the ratio of ^{13}C− secondary ions to ^{12}C− secondary ions in lipid droplets and within the capillaries of BAT (C) and heart (F). Areas of interest (eg, lipid droplets and capillary lumen) were examined pixel by pixel, and the ^{13}C/^{12}C ratios were calculated. Scale bar: 2 μm (A and B); 4 μm (C and D). Reproduced, with permission, from an article in the *Journal of Lipid Research* by Jiang *et al*.[20] BAT, brown adipose tissue; L, capillary lumen; LD, lipid droplets (white arrows); NanoSIMS, nanoscale secondary ion mass spectrometry; RBC, red blood cell.

role of CD36 in moving fatty acids across capillary endothelial cells needs more study. CD36 is expressed at high levels on capillary endothelial cells, and we suspect that this molecule could play a key role in binding the fatty acid products of TRL processing and then moving them across endothelial cells. If this were the case, we suspect that the CNBEI approach will allow us to visualize fatty acids within transcytotic vesicles of endothelial cells in wild-type mice, but not in CD36 knockout mice.

The CNBEI approach should also make it possible to visualize the distribution of lipids within cultured cells. For example, it should be possible to label cultured cells with (^{13}C)cholesterol and (^{2}H)choline (to label phosphatidylcholine) and then use the NanoSIMS data to quantify the amount of cholesterol, relative to phosphatidylcholine, in endoplasmic reticulum and Golgi membranes in response to metabolic and pharmacological interventions. The same cells should be useful for visualizing the distribution of cholesterol on the plasma membrane. A recent study by Das *et al*[25] proposed that there were three pools of cholesterol on the plasma membrane: a pool that is readily accessible to the cholesterol-binding protein PFO* (a mutant form of the bacterial toxin perfringolysin O), a sphingomyelin (SM)-sequestered pool that is accessible to PFO* only after sphingomyelinase treatment, and a pool that cannot bind PFO* even after sphingomyelinase treatment. At this point, it is unclear whether these different pools of cholesterol correspond to microdomains on the cell surface or whether those pools might correspond to identifiable features of the plasma membrane (as assessed by scanning electron microscope imaging). In the future, we can imagine using NanoSIMS to assess the binding of (^{15}N)PFO* to cells that have been grown in the presence of (^{18}O)cholesterol. It is conceivable that NanoSIMS imaging of ^{15}N and ^{18}O would allow one to identify 'PFO*-accessible' microdomains on the plasma membrane—regions that stand out above a more uniform distribution of (^{18}O)cholesterol. The NanoSIMS studies by Mary Kraft's laboratory suggested that SMs are enriched in specific regions of the plasma membrane of NIH 3T3 fibroblasts, whereas cholesterol is distributed more homogeneously.[19] In the future, NanoSIMS studies should allow investigators to simultaneously image cholesterol, SMs, PFO* binding, and the binding of lysenin (a sphingomyelin-binding protein)[26] on the surface of the plasma membrane.

CONCLUDING REMARKS

We developed a new approach, CNBEI, that is useful for visualizing stable isotope-labeled lipids at a subcellular resolution. The combined use of BSE and NanoSIMS imaging makes it possible to correlate the *chemical information* from the NanoSIMS with *subcellular morphological features* of the BSE images. An attractive feature of the CNBEI method is the ability to quantify the amount and distribution of a lipid, relative to another lipid or protein, in specific subcellular structures.

Funding National Heart, Lung, and Blood Institute (F32HL132471-01; HL090553; HL125335).

Competing interests None declared.

Provenance and peer review Commissioned; externally peer reviewed.

REFERENCES

1 Ikonen E, Blom T. Lipoprotein-mediated delivery of BODIPY-labeled sterol and sphingolipid analogs reveals lipid transport mechanisms in mammalian cells. *Chem Phys Lipids* 2016;194:29–36.
2 Maier O, Oberle V, Hoekstra D. Fluorescent lipid probes: some properties and applications (a review). *Chem Phys Lipids* 2002;116:3–18.
3 Hölttä-Vuori M, Uronen RL, Repakova J, *et al*. BODIPY-cholesterol: a new tool to visualize sterol trafficking in living cells and organisms. *Traffic* 2008;9:1839–49.
4 Marks DL, Bittman R, Pagano RE. Use of Bodipy-labeled sphingolipid and cholesterol analogs to examine membrane microdomains in cells. *Histochem Cell Biol* 2008;130:819–32.
5 Wu H, Volponi JV, Oliver AE, *et al*. In vivo lipidomics using single-cell Raman spectroscopy. *Proc Natl Acad Sci USA* 2011;108:3809–14.
6 Czamara K, Majzner K, Pacia M, *et al*. Raman spectroscopy of lipids: a review. *J Raman Spectrosc* 2015;46:4–20.
7 Passarelli MK, Winograd N. Lipid imaging with time-of-flight secondary ion mass spectrometry (ToF-SIMS). *Biochim Biophys Acta* 2011;1811:976–90.
8 Opilik L, Bauer T, Schmid T, *et al*. Nanoscale chemical imaging of segregated lipid domains using tip-enhanced Raman spectroscopy. *Phys Chem Chem Phys* 2011;13:9978–81.
9 Suga K, Yoshida T, Ishii H, *et al*. Membrane surface-enhanced Raman spectroscopy for sensitive detection of molecular behavior of lipid assemblies. *Anal Chem* 2015;87:4772–80.
10 Bich C, Touboul D, Brunelle A. Cluster TOF-SIMS imaging as a tool for micrometric histology of lipids in tissue. *Mass Spectrom Rev* 2014;33:442–51.
11 Alfonso-García A, Pfisterer SG, Riezman H, *et al*. D38-cholesterol as a Raman active probe for imaging intracellular cholesterol storage. *J Biomed Opt* 2016;21:061003–3.
12 Wei L, Yu Y, Shen Y, *et al*. Vibrational imaging of newly synthesized proteins in live cells by stimulated Raman scattering microscopy. *Proc Natl Acad Sci U S A* 2013;110:11226–31.
13 Jiang H, Favaro E, Goulbourne CN, *et al*. Stable isotope imaging of biological samples with high resolution secondary ion mass spectrometry and complementary techniques. *Methods* 2014;68:317–24.
14 Kleinfeld AM, Kampf JP, Lechene C. Transport of 13 C-oleate in adipocytes measured using multi imaging mass spectrometry. *J Am Soc Mass Spectrom* 2004;15:1572–80.
15 Steinhauser ML, Bailey AP, Senyo SE, *et al*. Multi-isotope imaging mass spectrometry quantifies stem cell division and metabolism. *Nature* 2012;481:516–19.
16 Senyo SE, Steinhauser ML, Pizzimenti CL, *et al*. Mammalian heart renewal by pre-existing cardiomyocytes. *Nature* 2013;493:433–6.
17 Baboo S, Bhushan B, Jiang H, *et al*. Most human proteins made in both nucleus and cytoplasm turn over within minutes. *PLoS ONE* 2014;9:e99346.
18 Frisz JF, Klitzing HA, Lou K, *et al*. Sphingolipid domains in the plasma membranes of fibroblasts are not enriched with cholesterol. *J Biol Chem* 2013;288:16855–61.
19 Frisz JF, Lou K, Klitzing HA, *et al*. Direct chemical evidence for sphingolipid domains in the plasma membranes of fibroblasts. *Proc Natl Acad Sci USA* 2013;110:E613–22.
20 Jiang H, Goulbourne CN, Tatar A, *et al*. High-resolution imaging of dietary lipids in cells and tissues by NanoSIMS analysis. *J Lipid Res* 2014;55:2156–66.
21 Goulbourne CN, Gin P, Tatar A, *et al*. The GPIHBP1–LPL complex is responsible for the margination of triglyceride-rich lipoproteins in capillaries. *Cell Metab* 2014;19:849–60.
22 Fong LG, Young SG, Beigneux AP, *et al*. GPIHBP1 and plasma triglyceride metabolism. *Trends Endocrinol Metab* 2016;27:455–69.
23 Scow RO, Blanchette-Mackie EJ, Smith LC. Role of capillary endothelium in the clearance of chylomicrons. A model for lipid transport from blood by lateral diffusion in cell membranes. *Circ Res* 1976;39:149–62.
24 Goldberg IJ, Eckel RH, Abumrad NA. Regulation of fatty acid uptake into tissues: lipoprotein lipase-and CD36-mediated pathways. *J Lipid Res* 2009;50:S86–90.
25 Das A, Brown MS, Anderson DD, *et al*. Three pools of plasma membrane cholesterol and their relation to cholesterol homeostasis. *Elife* 2014;3:e02882.
26 Yamaji A, Sekizawa Y, Emoto K, *et al*. Lysenin, a novel sphingomyelin-specific binding protein. *J Biol Chem* 1998;273:5300–6.